VII International Conference on Computational Methods in Marine Engineering
MARINE 2017
M. Visonneau, P. Queutey and D. Le Touzé (Eds)

DISCRETE ELEMENT METHOD SIMULATION OF A SPLIT HOPPER DREDGER DISCHARGING PROCESS

Josip Basic*, Dario Ban*, Nastia Degiuli† and Nicolin Govender‡

* Faculty of Electrical Engineering, Mechanical Engineering and Naval Architecture
University of Split, Rudera Boskovica 32, Split, Croatia
e-mail: jobasic@fesb.hr, dario.ban@fesb.hr - Web page: www.fesb.hr

† Faculty of Mechanical Engineering and Naval Architecture
University of Zagreb, Ivana Lucica 5, Zagreb, Croatia
e-mail: nastia.degiuli@fsb.hr - Web page: www.fsb.hr

‡ Advanced Mathematical Modeling CSIR
Meiring Naude Road, Pretoria, South Africa
e-mail: govender.nicolin@gmail.com - Web page: www.csir.co.za

Key words: Discrete Element Method, Radial Basis Function, Polynomial RBF, Ship Stability

Abstract. Split Trailing Suction Hopper Dredgers (Split TSHD) have longitudinally-split hull, which symmetrically opens when executing gravity-driven unloading of the cargo, while being exposed to various environmental conditions. Even though they have variable hull geometry, their hydrostatic and stability characteristics are usually calculated for initial and unchanged loading conditions only, which is a requirement imposed by classification society stability regulations for TSHD ships [2, 3, 4]. In order to investigate the significance of the discharge process dynamics on actual ship stability, unsteady numerical simulations were performed with the Discrete Element Method (DEM) for symmetrical hopper opening during cargo discharge procedure, without the hull opening failure modes examined. The ship hydrostatic properties, which are pre-calculated analytically using Radial Basis Functions (RBF) for all possible states [11], are used in combination with the solver in order to compute the righting moment and the righting arm, which are affected by the dynamics of the cargo and the loss of displacement. The dynamics of the cargo discharge process was simulated with a DEM solver implemented for Graphics Processing Units (GPUs), Blaze-DEMGPU [8]. Spherical shapes of particulate elements were employed to model the soil cargo, with both cohesion and buoyancy effects included for wetted elements. The simulations of the discharging were performed for various loading conditions. Numerical simulations indicate that the dynamics of the cargo during its discharging should not be ignored due to its effect on the transverse stability of the ship. Therefore, an incoming wave and other environmental loads in combination with a hull opening failure during the discharge could lead to inapt unstable situation of the ship. Non-symmetrical Split TSHD ship openings will be examined in future work, with an investigation of its influence on ship stability and safety of cargo discharge procedures in failure modes.

1 INTRODUCTION

Trailing Suction Hopper Dredgers (TSHDs) excavate large amounts of material from the sea floor and they transport the material to another place. A special type of a dredger ship called Split Trailing Suction Hopper Dredger (Split TSHD) is build with longitudinally-split hull, which opens to perform gravity-driven cargo discharging process, as depicted in Figure 1. The main advantage of the Split TSHD is the fast cargo discharge on a certain near shore position, using mass flow from the silo-shaped cargo hold. Split TSHDs have both sides connected by hinges and the opening is controlled with hydraulic cylinders. While discharging the cargo, failure

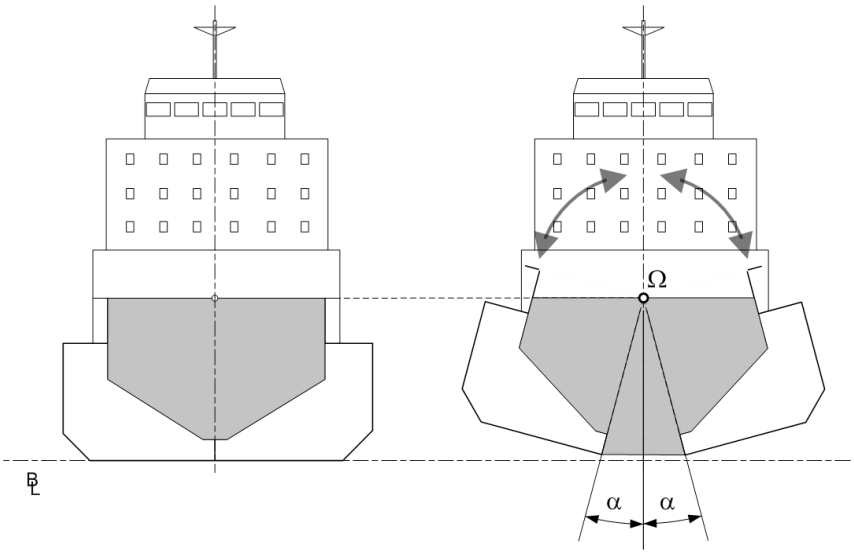

Figure 1: Split TSHD main frame section, with split hulls in a discharge condition rotated around the joint

of the main electric power supply and/or the main hydraulic unit and/or single failure of the normal control systems can occur. Furthermore, as the two halves of split hopper hull are only connected with the hinges and cylinders, a single failure of each of these elements could lead to a catastrophic failure [1]. These opening failures can produce non-symmetric ship geometry, with high risk of reduced ship stability that should be assessed. Moreover, initially trapped water or water that leaped above the freeboard negatively impacts the stability particulars, as it is located at a relatively high position (increasing the ship's centre of gravity and decreasing the initial metacentric height) and may be associated with an additional free surface moment [1]. The shifting of the cargo can have major effect on the stability of a ship, and usually it is not taken into account for the stability and seakeeping calculations, but the ship construction and its cargo are considered as one rigid body. On the other hand, sandy and gravel cargoes that TSHDs are carrying are not constrained to the ship construction and are submissive to rapid movements. A schematic view of the mass flow in the process of emptying the hopper, while the ship draught is rapidly reduced is shown in Figure 2. The cargo shape, a hull opening malfunction and external loads (wind, waves, trapped water, etc.) can cause force concentration of one side of the hopper and reduce the ship stability in this process. Usual hydrostatic and stability calculations

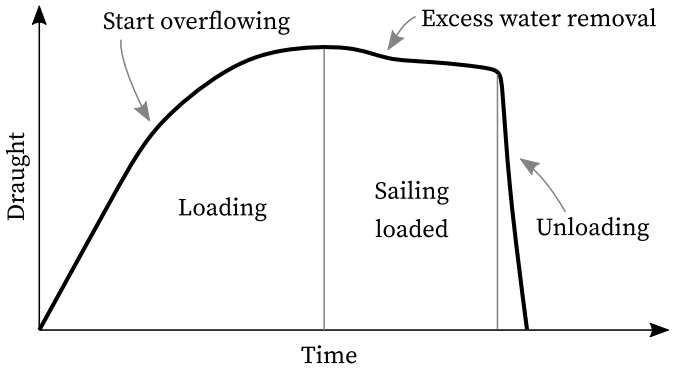

Figure 2: A schematic view of the change in draught of a TSHD in service

are conducted for initial, non-variable hull geometries. Current stability regulations regarding Split TSHDs [2, 3, 4] cover initial loading conditions thus avoiding intermediate ship positions and belonging hydrostatic particulars calculations. However, full numerical calculations must overcome complexities of defining the variable ship geometry for the range of opening angles, and calculation of belonging hydrostatic particulars for the each case. Efficient solutions for these ship geometry variations are analytical geometry description methods. An analytical solution of the ship geometry description based on polynomial RBFs (PRBFs) [5, 6] is used in this study. The calculation of hydrostatic calculations for arbitrary heel angles is enabled based on [7], which enables hull affine geometry transformations using rotation, needed for the description of a opened Split TSHD. Moreover, all theoretical ship hydrostatic particulars are pre-calculated in advance for all possible loading conditions, containing three degrees of freedom for a quasi-static ship condition of the draught, the angle of trim and the heel angle [11].

In order to investigate the significance of the discharge process dynamics on actual ship stability, Discrete Element Method (DEM) unsteady numerical simulations were performed for hopper opening during the cargo discharge procedure, without the hull opening failure modes examined. The dynamics of the cargo discharge process was simulated with a DEM solver implemented for Graphics Processing Units (GPU), Blaze-DEM [8, 12]. Spherical elements were used to model the soil cargo, with both cohesion and buoyancy effects included for the wetted elements. Simulations of the cargo discharging were performed for various loading conditions. Ship hydrostatic properties are pre-calculated analytically for all possible states and coupled with the solver to compute ship motions caused by the dynamics of the cargo and the loss of displacement. The paper is organized as follows. The numerical methodology divided into three segments is presented in Section 2. The simulated problem is described in Section 3. The results are presented and discussed in Section 4. Finally, conclusions are drawn in Section 5.

2 NUMERICAL METHODOLOGY

The numerical calculation methodology is divided into three segments. Firstly, theoretical ship hydrostatic particulars are precalculated with RBFs in advance, for all possible states. Secondly, the DEM solver is used to fill the hopper with cargo, and to simulate the cargo unloading while opening the longitudinally split hopper. The simulations are done for various heeling scenarios.

And thirdly, unsteady loads from the discrete elements on the hull geometry are analysed in time, in order to find the worst case of undesirable angular momentum for the simulated case.

2.1 Discrete Element Method

The linear momentum of a particle i is given by:

$$\boldsymbol{L}_i = m_i \boldsymbol{v}_i \tag{1}$$

where m_i and $\boldsymbol{v}_i$ are the mass and the velocity of a particle i, respectively. The angular momentum of a particle i is given by:

$$\boldsymbol{H}_i = \boldsymbol{I}_i \boldsymbol{\omega}_i \tag{2}$$

where $\boldsymbol{I}_i$ is the inertia tensor, and $\boldsymbol{\omega}_i$ is the angular velocity of the particle. Given that all forces $\boldsymbol{F}_i$ and torques $\boldsymbol{T}_i$ act on i-th particle, the problem is reduced to the integration of the change in the linear momentum:

$$\dot{\boldsymbol{L}}_i = m_i \frac{\mathrm{d}^2 \boldsymbol{x}_i}{\mathrm{d}t^2} = \boldsymbol{F}_i \tag{3}$$

and the integration of the change in the angular momentum for an axis fixed to the body:

$$\dot{\boldsymbol{H}}_i = \boldsymbol{I}_i \frac{\mathrm{d}\boldsymbol{\omega}_i}{\mathrm{d}t} + \boldsymbol{\omega}_i \times \boldsymbol{H}_i = \boldsymbol{T}_i \tag{4}$$

where $\boldsymbol{x}_i$ is the position of i-th particle. A linear and an angular position of a particle, and its velocity and acceleration are obtained after the integration. Forces $\boldsymbol{F}_i$ consist of the surface traction and body forces, and torques $\boldsymbol{T}_i$ are calculated based on the surface traction forces. The surface traction on a particle i are the result of contacts with other particles, contacts with boundaries of the domain or applied external loads. An assumption in many DEM simulations is that particles are considered to be rigid for the duration of collision contacts, since the deformations occur on a time scale which is much smaller than what is required for capturing the macroscopic behaviour of a system. The interaction forces between particles i and j in contact is resolved through constitutive relationship of a linear repulsive force, and a linear dissipative force model, given by:

$$f_{ij} = k\delta_{ij} + \gamma_0 \dot{\delta}_{ij} \tag{5}$$

where δ_{ij} is the contact distance, $\dot{\delta}_{ij}$ is the velocity with which the contact distance changes, k (N/m) is the normal contact stiffness, and γ_0 is the normal contact damping. The friction resistance as a result of sliding due to the relative tangential surface velocity $\boldsymbol{v}_{ij}^t$ between particles i and j in contact is resolved as:

$$\boldsymbol{v}_{ij}^t = \boldsymbol{v}_{ij} - \boldsymbol{n}_{ij} \left(\boldsymbol{n}_{ij} \cdot \boldsymbol{v}_{ij} \right) \tag{6}$$

which depends on the relative surface velocity $\boldsymbol{v}_{ij}$ between particles and the contact normal $\boldsymbol{n}_{ij}$. The relative surface velocity at the point of contact is due to the relative translation and rotation of the two particles:

$$\boldsymbol{v}_{ij} = \boldsymbol{v}_i - \boldsymbol{v}_j + \boldsymbol{r}_i \times \boldsymbol{\omega}_i + \boldsymbol{r}_j \times \boldsymbol{\omega}_j \tag{7}$$

where $\boldsymbol{r}_i$ is the vector from particle centre of mass to the contact point. The relative tangential surface velocity $\boldsymbol{v}_{ij}^t$ in addition to Coulomb's law dictates the tangential force with direction such that it opposes the motion of the two particles. A drawback of the DEM is the large computational cost of collision detection, which scales with the number of particles and geometric complexity. Therefore, particle shapes are mostly approximated with a sphere, although polyhedral shaped particles can capture real particle shape without introducing non physical artefacts.

In this study, Blaze-DEM solver [8] is employed for the dynamic simulation of hull opening and the cargo discharge process. Blaze-DEM is a modular GPU based discrete element method (DEM) framework that supports polyhedral shaped particles by employing a ray-tracing type methodology. On a modern GPU (nVidia GTX 980 Ti), one time step take of a DEM solver takes around ten milliseconds for one million of particles. Usual time step needed for the simulation to be stable is around $\Delta t < 10^{-3}$ s.

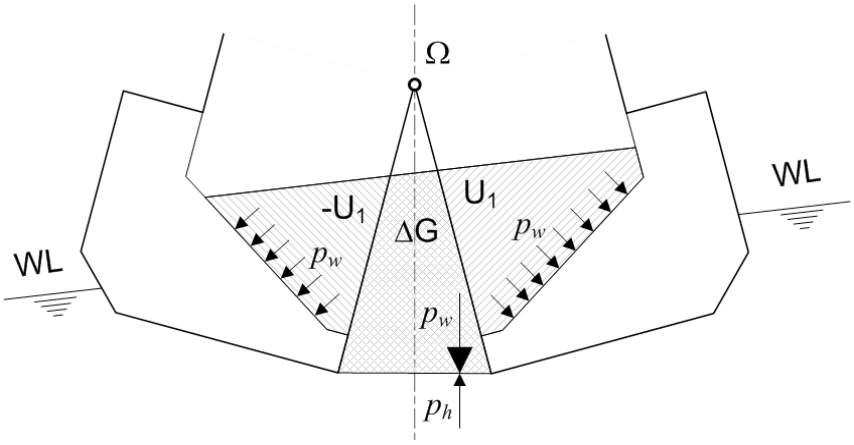

Figure 3: Schematic view of cargo pressure acting on the hopper

2.2 Hydrostatic Particulars Using RBFs

It is shown in [5] that 2D ship geometry with discontinuities can be described using the composition of cubic and linear PRBFs, thus enabling further solutions of basic ship hydrostatic integrals, necessary for further stability calculations [7]. The main advantage of PRBFs over other description methods is the possibility of an analytical description of a curve with discontinuities. The composition of linear and cubic PRBFs with dense distribution of points around discontinuities is exact solution of one-dimensional discontinuity description problem with

$$f(x) = \sum_i w_i |x - t_i|^3 + \sum w_l |x - t_l| + c \tag{8}$$

where w is the weight of a point, t is the point position vector, i is the point in the input data set, l is the point in the set of discontinuity data set, c is the shape parameter. After the geometry is globally described using the composition of a cubic and a linear polynomial RBF, hydrostatic particulars of a semi-immersed body can be calculated directly, together with

belonging particulars for arbitrary orientation of the body. Complete hydrostatic particulars, for the outer as well as for the inner ship geometry, can be calculated for the specified range of drafts and heel angles. Interested readers are referred to [7, 11] for the complete explanation of the methodology.

Length, overall, L_{OA}	98.0 m
Breadth, B	18.5 m
Draught, max, T	6.55 m
Hopper capacity, V_h	4700 m^3
Hopper length, L_h	52 m
Deadweight, DWT	6 000 t
Speed, loaded, v	12 knots
Propulsion engines power, P_B	2 x 3300 kW
Hull opening angle, α	13°, for each side
Hull opening time, t_α	~ 45 s

Table 1: Main ship particulars

2.3 Cargo Dynamics and Transverse Stability

The forces that discrete elements impose on the hopper tank are summed for each time-step while the simulation is being performed, as shown in Figure 3. One-way quasi-static coupling is considered, such that for each DEM simulation step, hydrostatic particulars are analysed, i.e. read for the pre-calculated database. The value of the dynamic righting arm is obtained as:

$$GZ\left(t\right) = \frac{RM\left(t\right)}{F\left(t\right)}, \tag{9}$$

where RM is the righting moment, and F is the resultant force vector calculated by summing all relevant forces of the free body. Total mass and its centroid is obtained for each time instant as a combination of time-invariant mass of the ship without the cargo, and the mass of the cargo left in the hopper. The immersed volume centroid and buoyancy force value for the current heel angle of the ship is obtained directly by reading pre-calculated database explained in Section 2.2. Therefore, the righting arm for a specific time instant $GZ\left(t\right)$ can be calculated from Eq. (9)., based on the ship weight, the cargo weight and dynamic forces, buoyancy forces, and the calculated mass and the centre of mass. If it is considered that the change of the shape of the ship in the vicinity of the waterline does not happen abruptly, metacentric height for small angles of heel can be expressed in the following way:

$$GM\left(t\right) = GZ\left(t\right)\sin\varphi. \tag{10}$$

Parameter	Gravels	Sands
Specific gravity	2.5 - 2.8	2.6 - 2.7
Bulk density (t/m^3)	1.45 - 2.30	1.40 - 2.15
Dry density (t/m^3)	1.40 - 2.10	1.35 - 1.90
Void ratio	0.25 - 1.0	0.30 - 0.54
Angle of internal friction (°)	35 - 45	32 - 42
Permeability (m/s)	> 0.01	10^{-7} - 10^{-3}

Table 2: Indicative values of soil properties for cohesionless gravels and sands

3 THE PROBLEM DESCRIPTION

3.1 The Ship

The main characteristic of a Split TSHD that makes that kind of ship different than other ship types, is that her geometry is not constant during the unloading process. Her outer and/or inner compartments change in time; inner compartments except cargo hold remain with constant geometry. The ship modelled in this study has three inner compartments on the main frame section: one symmetric cargo hold and two equal ballast tanks on each side of the ship, symmetrically and transversely positioned about the centreline plane. Main particulars of the ship considered in this study are given in Table 1. The filling of ballast water in the discharge process is ignored, since the hull opening time is relatively short compared to the pumps flow rate.

3.2 The Cargo

While describing the size and the shape of grains in granular soils, only predominant size and shape ranges need to be mentioned. To include in the description the full range of every particle present is unhelpful as the size and shape descriptors quickly become so broad as to be meaningless (e.g. nearly all sand becomes "fine to coarse" and nearly all gravel becomes "angular to rounded") [9]. Soil properties can vary over a range but they do have typical values. Table 2 provides examples of values for gravels and sands soil properties, based on [10], which are used as solver input parameters. Of course, properties can be outside the indicated ranges, but the table is indicative of typical ranges. Typical particle size distributions for the marine dredging process taken from [9] are shown in Figure 4. Specimen #4 is used as the simulation input, which is described as silty very sandy gravel, where gravel is fine to medium and sand is medium to coarse. Even though the Blaze-DEM solver used for the dynamic simulation offers novel and fast method for large-scale polyhedral elements described in [13], spherical elements were employed for the discretisation of the cargo, due to their efficiency and high number of performed runs. Each simulation is firstly initialized by a velocity inlet rectangle, positioned above the hopper tank. Discrete elements of various sizes are randomly spawned, based on the distribution shown in Figure 4, and discharged through the inlet to gravitationally fill the compartment. After the cargo movement has stabilized, hull is being opened, force from the mass flow is analysed by summing forces on the compartment, and stability calculations are performed. An example of filled hopper with randomly distributed particle types, ready to be discharged, is show in Figure 5. For the presented case, hopper is filled with around 2 million particles that have total mass of

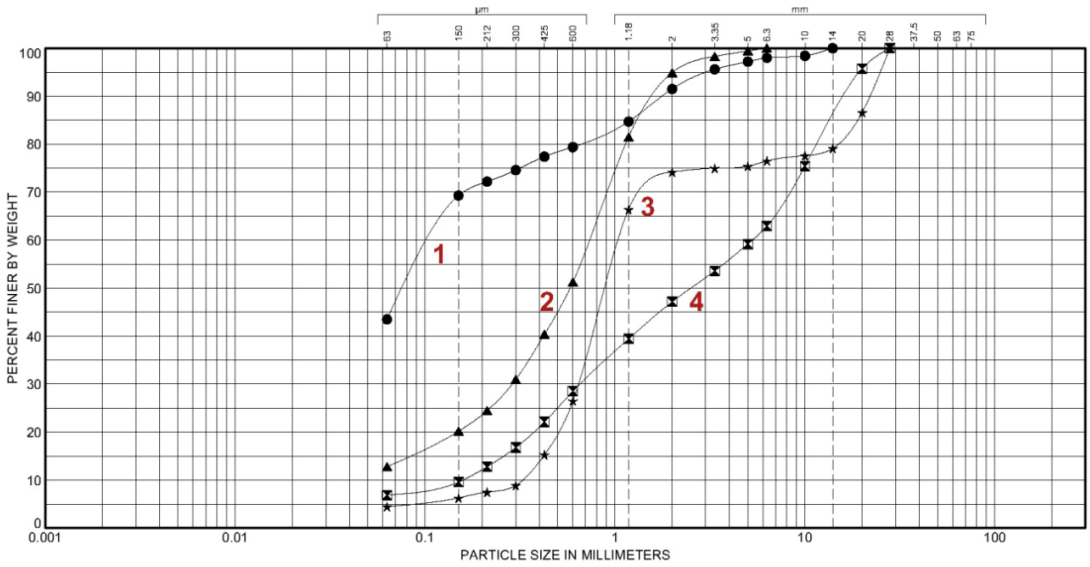

CLAY	SILT			SAND			GRAVEL			COBBLES
	fine	medium	coarse	fine	medium	coarse	fine	medium	coarse	

Specimen ID	Description Using BSI Classification	LL	PL	PI	%Gravel	%Sand	%Fines
● 1	sandy CLAY, sand is fine	36	18	18	8.5	48.0	43.5
▲ 2	gravelly clayey SAND, sand is medium to coarse, gravel is fine	38	20	18	5.1	82.1	12.8
★ 3	slightly clayey very gravelly SAND, sand is medium to coarse, gravel is medium to coarse	35	22	13	25.8	69.7	4.5
⧓ 4	silty very sandy GRAVEL, gravel is fine to medium, sand is medium to coarse	42	29	13	52.8	40.3	6.9

Figure 4: Particle size distributions and specimen descriptions [9]

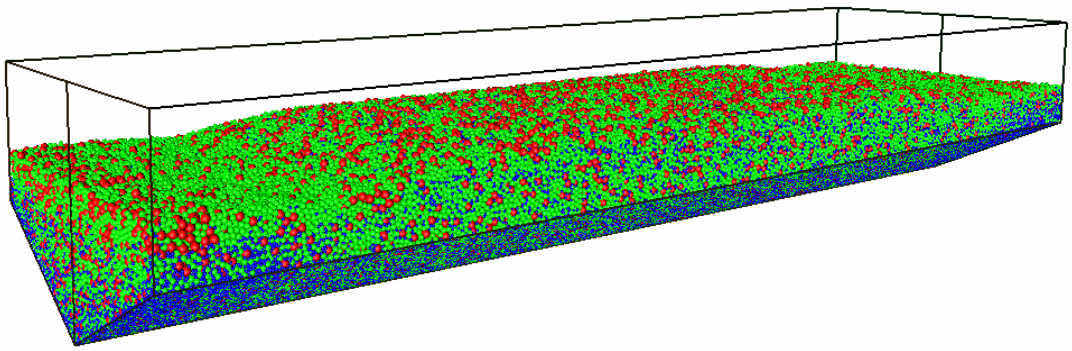

Figure 5: Gravitationally filled cargo compartment, 6000 tons of medium gravel and coarse sand, represented with with 2 million particles

6000 t. The particles are coloured by their diameter, from largest to smallest: red, green, blue and yellow. For the most realistic modelling of the cargo, 10+ millions of particles are needed. For the approximation, smallest particles that do not contribute greatly with their mass can be ignored, i.e. substituted by adding some more of the larger particles to compensate for the mass lost by ignoring the smallest particles.

4 RESULTS AND DISCUSSION

Blaze-DEM solver is validated against hopper flow experiments for both polyhedra and spherical particles [12], and an excellent agreement is found in both the flow-rate and pattern of the particles. For non-cohesive particles without the effects of buoyancy included, the fully loaded ship described in Section 4.1 discharges the cargo in about 25 s. With the mentioned effects included, the discharge procedure takes up to 35 s, which is slightly less then reported by ship specifications. The discrepancy can mostly be attributed to the usage of spherical elements instead of more realistic polyhedrals. Two time instants of the discharging process are rendered in Figure 6, with coloured velocities of the particles. Rolling motion of the ship up to heel angle of

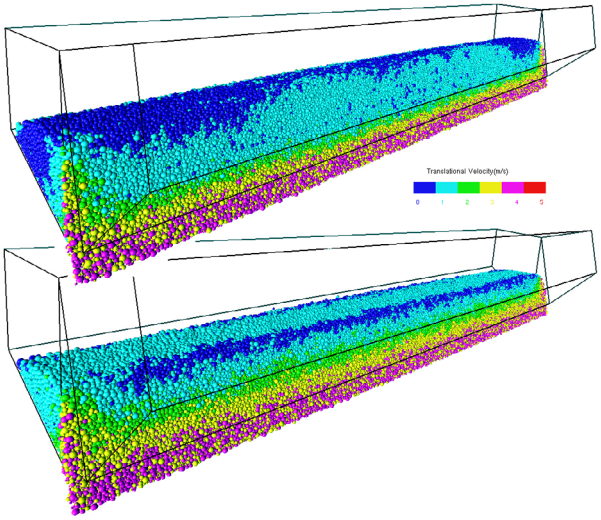

Figure 6: Two time instants of the gravitational hopper discharge

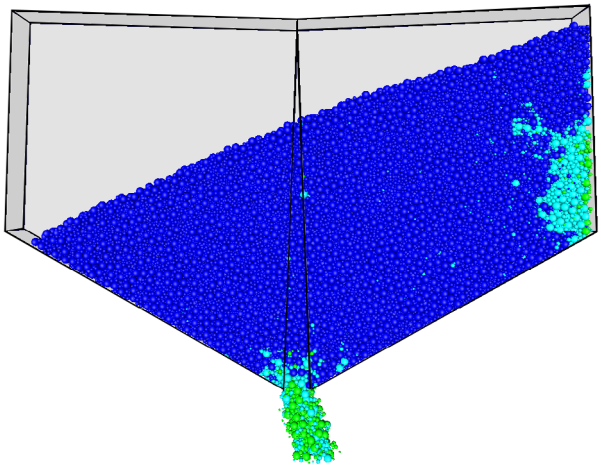

Figure 7: Hopper section of 1 m length, for the heel angle of 20°

20° did not yield significant difference in overall time needed for the cargo to discharge. Therefore, it can be said that the ship displacement at specific time instant is similar for various simulations of the specific loading case, i.e. for initially set displacement $\nabla(t=0)$. Therefore, in order to simplify the numerical procedure and to perform inapt loading scenarios, each simulation was executed for the ship for target heel angle where the cargo would slightly tilt and move its centre of mass, in order to analyse righting arm that is dynamically changing in time. The section cut of a simulation is shown in Figure 7. Ship is allowed to roll around the target heel angle, due to non-symmetrical transverse weight distribution along with unsteady forces from the particles acting on hull. Generally, the centre of mass is dynamically changing, and the resultant force and the moment of force is calculated by summing the ship, cargo and buoyancy components, which are used to derive the value of the righting arm for each discrete time instant, as explained in Section 2.3. The righting arm values calculated with Eq. (9) are presented in Figure 8, in the classic sense as if the remaining cargo at a time instant t represents a loading case. Obviously, a critical scenario occurs when the cargo in fully loaded hopper tilts with the ship heel angle, and thus moves centre of mass away from the centreplane. The righting arm reaches negative

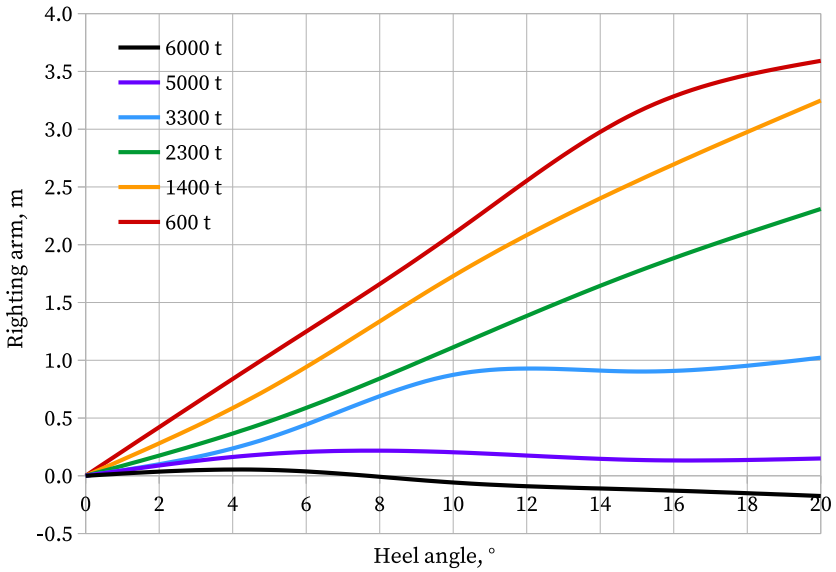

Figure 8: Dynamic righting arm values for various mass of cargo remaining in the hopper

value at 8° of the heel angle, but the loads needed for that heel angle to occur are out of scope of this study. In addition, granular cargo cohesion and inertia help that the cargo tilting does not happen instantly. It can be deduced that relatively impulsive cargo shifting, or imbalanced loading from the start for the fully loaded case has negative impact on the ship stability. The ship can recover its stability by moving the buoyancy centroid with further opening the hopper and by decreasing the draught with the discharging of the cargo. The metacentric height is straightforwardly calculated with Eq. (10) and plotted in Figure 9. Since the ship rolling is allowed around the target heel angle, the obtained roll angle of the ship (around the target heel angles) is shown in Figure 10.

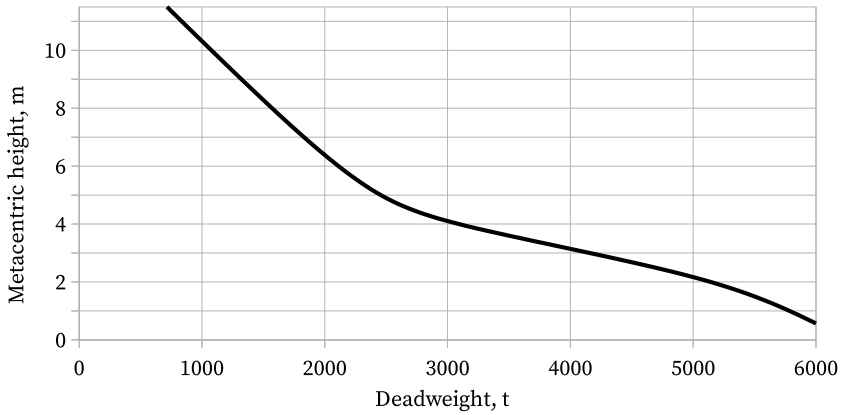

Figure 9: The metacentric height GM values for various mass of cargo remaining in the hopper

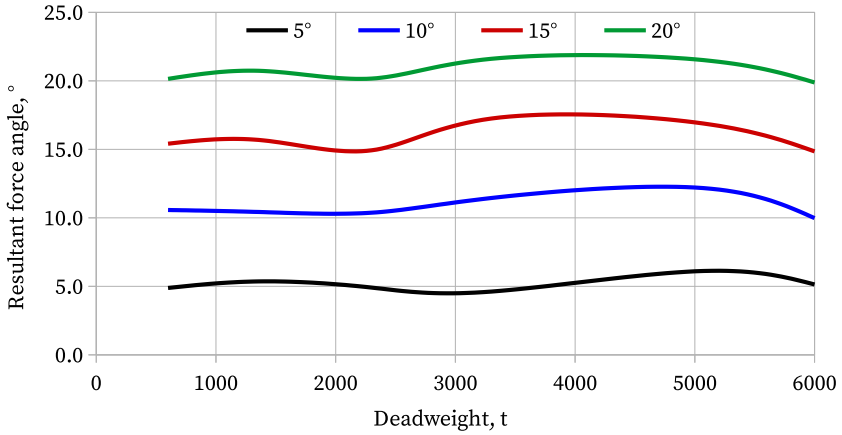

Figure 10: The angle of total force of cargo applied on the hull, compared to the heel angle

5 CONCLUSIONS

Problems that can be modelled and solved with the DEM, can efficiently be simulated on modern hardware by employing data-parallel algorithms. Blaze-DEM solver used in this study can simulate over 10 millions of spherical or polyhedral particles on one GPU device, thus enabling relatively fast simulations of cohesive and non-cohesive granular soils used in maritime dredging processes, e.g. silt, sand and gravel and cobbles.

Split TSHD ship that excavates and carry such materials, symmetrically opens up its longitudinally split hull to perform gravity-driven cargo discharging process. This mass flow in a silo-shaped cargo hold is eligible to simulate with DEM. Even though such ships are exposed to various environmental conditions while opening, their hydrostatic and stability characteristics are usually calculated for initial and unchanged loading conditions only. In this work, unsteady DEM solver was coupled with RBF ship stability solver in order to investigate the significance of the Split TSHD discharge process dynamics on its stability.

Simulations were performed for various heel angles of the ship, where the granular cargo would shift to the heeling side, and hopper would open with defined angular speed. Resultant force and moment of force were calculated by summing the ship, cargo and buoyancy components, which were used to derive the value of righting arm for each discrete time instant. The results showed that relatively impulsive cargo shifting, or imbalanced loading from the start for the fully loaded case has negative impact on the ship stability. Such TSHD ship recovers its stability by further opening the hopper (moving the buoyancy centroid) and discharging cargo (decreasing the draught).

Albeit these kind of ships operate mostly near shore, environmental conditions can be harsh. This raises a question whether a disaster can occur for non-symmetrical hopper section caused by hull opening failure in combination with an incoming wave and other loads (e.g. wind, free-surface effects), which will be examined in future work.

REFERENCES

[1] G. de Jong, Classification of Dredgers - Technical & Regulatory Developments, Bulletin Technique, Bureau Veritas, 2010.

[2] Bureau Veritas, Rules for the Classification of Steel Ships, Pt. B, Ch. 3, App. 2, Dredgers, 2016.

[3] Bureau Veritas, Rules for the Classification of Steel Ships, Pt. D, Ch. 13, Sec. 2, Ships for Dredging Activity - Hull and Stability, 2016.

[4] International Maritime Organization, Guidelines for the construction and operation of dredgers assigned reduced freeboard, Circular letter No. 2285, 2001.

[5] D. Ban, B. Blagojević and B. Čalić, "Analytical solution of global 2D description of ship geometry with discontinuities using composition of polynomial radial basis functions", Journal of Naval Architecture and Shipbuilding Industry, 65(2), pp. 1-22, (2014).

[6] D. Ban and B. Ljubenkov, "Global ship hull description using single RBF", 16th International Congress of the International Maritime Association of the Mediterranean. Pula, Croatia. (2015).

[7] Ban D. and Bašić J., "Analytical solution of basic ship hydrostatic integrals using polynomial radial basis functions", Journal of Naval Architecture and Shipbuilding Industry, 66(3), pp. 15-37, (2015).

[8] N. Govender, D.N. Wilke and S. Kok, "Blaze-DEMGPU: Modular high performance DEM framework for the GPU architecture", SoftwareX, dx.doi.org/10.1016/j.softx.2016.04.004, (2016).

[9] MarCom Working Group, Classification of Soils and Rocks for the Maritime Dredging Process, Report no. 144, World association for Waterborne transport infrastructure, 2014.

[10] F.G. Bell, "Engineering Properties of Soils and Rocks", Butterworth & Co, London, 1981.

[11] D. Ban, J. Basic and D. Dobrota, “Split TSHD Hydrostatic Particulars Calculation for Cargo Discharge Procedure using Polynomial RBFs”, Journal of Marine Science and Application, pp. 1-23, (2017).

[12] N. Govender, P. Pizette, D.N. Wilke and N-e. Abriak, “Validation of the GPU Based Blaze-DEM Framework for Hopper Discharge”, IV International Conference on Particle-based Methods, Barcelona, Spain, (2015).

[13] D.N. Wilke, N. Govender, P. Pizette, N-e. Abriak, “Computing with Non-convex Polyhedra on the GPU”, 7th International Conference on Discrete Element Methods, Dalian, China, (2016).